AIP | Applied Physics Letters

Determining conductivity and mobility values of individual components in multiphase composite Cu1.97Ag0.03Se

Tristan W. Day, Wolfgang G. Zeier, David R. Brown, Brent C. Melot, and G. Jeffrey Snyder

Citation: Applied Physics Letters **105**, 172103 (2014); doi: 10.1063/1.4897435
View online: http://dx.doi.org/10.1063/1.4897435
View Table of Contents: http://scitation.aip.org/content/aip/journal/apl/105/17?ver=pdfcov
Published by the AIP Publishing

Determining conductivity and mobility values of individual components in multiphase composite $Cu_{1.97}Ag_{0.03}Se$

Tristan W. Day,[1] Wolfgang G. Zeier,[1,2] David R. Brown,[1] Brent C. Melot,[2] and G. Jeffrey Snyder[1,a)]
[1]*Department of Materials Science, California Institute of Technology, MC 309-81, Pasadena, California 91106, USA*
[2]*Department of Chemistry, University of Southern California, Seeley G. Mudd Bldg., 3620 McClintock Ave., Los Angeles, California 90089-1062, USA*

(Received 12 August 2014; accepted 22 September 2014; published online 28 October 2014)

The intense interest in phase segregation in thermoelectrics as a means to reduce the lattice thermal conductivity and to modify the electronic properties from nanoscale size effects has not been met with a method for separately measuring the properties of each phase assuming a classical mixture. Here, we apply effective medium theory for measurements of the in-line and Hall resistivity of a multiphase composite, in this case $Cu_{1.97}Ag_{0.03}Se$. The behavior of these properties with magnetic field as analyzed by effective medium theory allows us to separate the conductivity and charge carrier mobility of each phase. This powerful technique can be used to determine the matrix properties in the presence of an unwanted impurity phase, to control each phase in an engineered composite, and to determine the maximum carrier concentration change by a given dopant, making it the first step toward a full optimization of a multiphase thermoelectric material and distinguishing nanoscale effects from those of a classical mixture. © *2014 AIP Publishing LLC*.
[http://dx.doi.org/10.1063/1.4897435]

Great strides have been made in improving thermoelectric performance by combining solid phases. Microstructuring to scatter phonons while maintaining high carrier mobilities[1] is a proven method for reducing the lattice thermal conductivity.[2] The high potential for inclusions to improve the electronic properties of thermoelectrics by doping,[3,4] electron filtering,[5] and composition modulation[6] has lead to values of the thermoelectric figure of merit zT greater than unity, approximately the value needed for commercial modules.

The mechanisms described above use a second phase or microstructure to affect the performance of the matrix phase due to quantum mechanical or other nanometer size effects on the transport properties. This is because the zT of a composite material cannot be improved by the combination of two phases in a parallel, series, or arbitrary mixture which can be described by classical phenomena.[7] Secondary phases are also of concern because phase-pure synthesis of some materials is challenging, making measurement of the electronic properties of the target compound difficult.[8]

Interpretation of transport measurements of multiphase materials is critical for thermoelectric optimization and application; however, no one has demonstrated a method for separating the transport properties of each phase in a composite from measurements of the bulk material.

In this work, we seek to provide a method for extracting the conductivity and mobility of each phase in a composite from measurements of the in-line and Hall resistivity of the bulk, using effective medium theory. Effective medium theory can be used to derive expressions for two-phase transport properties of any kind, including the electrical conductivity,[7,9] the Seebeck coefficient,[7] and the thermal conductivity,[10,11] meaning that effective medium theory can be united with microstructure engineering to design electronically optimized, low lattice thermal conductivity thermoelectric materials. We take the first step toward such an optimization by applying Stroud's powerful coherent potential approximation[9] along with magnetic-field dependent resistivity measurements to determine the conductivity and mobility of each phase in a two-phase composite. Our approach does not include nanoscale effects, so it can also be used to distinguish between bulk and nanoscale contributions, or it can be used in conjunction with models of small-size properties, as some researchers have already done.[10]

This derivation yields quantitative correction terms that can be applied to analyze transport data. In many cases, this method would give quantitative justification for use of a single phase approximation. In other cases, this method will give a quantitative correction factor. The method also identifies the volume-fraction weighted Hall conductivity of the matrix phase and the magnetoresistance contribution of each phase as the critical scaling factors which ultimately determine what level of correction or even appropriateness a single phase transport model may have.

In general, the contribution of each phase in a composite to the magnetoresistance and to the Hall effect depends on its charge carrier mobility multiplied by the magnetic field strength. Because the dependence is nonlinear, we can use a magnetic field to distinguish the effect each phase has on electrical transport in a composite. $Cu_{1.97}Ag_{0.03}Se$ contains an impurity phase with a high mobility that exerts a disproportionate influence on the transport properties, providing us with a model system to show the viability of this approach.

X-ray diffraction data show that this composition comprises two phases, the matrix with the crystal structure of Cu_2Se and an impurity phase with the crystal structure of

a)Author to whom correspondence should be addressed. Electronic mail: jsnyder@caltech.edu.

CuAgSe, which dissolves into the matrix around 390 K.[12,13] The number of phases is confirmed by scanning electron microscopy (SEM) (inset of Figure 1), which shows the gray matrix phase and a light-colored impurity phase. The dark spots are voids; according to geometric density measurements, the sample has only 3% porosity. $Cu_{1.97}Ag_{0.03}Se$ displays unusual electrical properties below its superionic phase transition at 400 K (Figure 1). It has a Seebeck coefficient greater than zero indicating holes as the majority carriers, but a Hall coefficient R_H less than zero, indicating electrons have a strong influence on the electrical conductivity in this composite. This opposite behavior is rare in materials but occurs in some elemental metals like Li, Cu, Ag, and Au[14] and in some semiconductors such as $AgSbTe_2$ and in PbTe-PbS alloys.[15] In these cases, band structure effects can explain these properties.[16] However, in the case of $Cu_{1.97}Ag_{0.03}Se$, R_H becomes positive as soon as the impurity phase dissolves, suggesting that only the impurity phase is n-type with an electron mobility much greater than that of the matrix. Indeed, the CuAgSe impurity phase is n-type and has high mobility, around 2000 $cm^2\ V^{-1}\ s^{-1}$ at room temperature, two orders of magnitude greater than that of Cu_2Se, the apparent matrix phase.[17]

The lack of a fully confirmed crystal structure for the highly Cu-disordered Cu_2Se[18] and these conflicting carrier types make $Cu_{1.97}Ag_{0.03}Se$ a challenging material on which to develop an electrical transport model. The disparity of the electron mobility values between its phases makes it a perfect model system for the combination of magnetic-field dependent resistivity measurements and effective medium theory. This technique allows us to extract the resistivity tensor of each phase, the results of which we show below.

$Cu_{1.97}Ag_{0.03}Se$ was synthesized by the method in Day *et al.* and was characterized by powder X-ray diffraction.[13] SEM micrographs were taken on a JEOL JXA-8200 electron probe micro-analyzer.

The data in Figure 1 were taken on a custom-built Hall effect system with van der Pauw geometry and a magnetic field of +/−2 T.[19] The data in Figure 2 were taken on a Quantum Design Physical Property Measurement System (PPMS) with its stronger magnet and more sensitive measurements. The in-line resistivity ρ_{xx} and the Hall resistivity ρ_{yx} were measured by the four-point method with alternating current using the electrical transport option at a range of magnetic field strengths between 14 T and −14 T. Electrical leads were fixed to the sample using silver epoxy. A current of 10 mA and a frequency of 3 Hz were used to measure ρ_{xx}. A current of 4 mA and a frequency of 15 Hz were used to measure ρ_{yx}. These parameters yielded the smallest phase angles between the input current and output voltage for each measurement.

The measurements of ρ_{yx} are offset by a term that increases with magnetic field due to imperfect alignment of the voltage leads. Therefore, the ρ_{yx} data shown in this work were obtained by the following correction:[20]

$$\rho_{yx,data}(B) = \rho_{yx,measured}(B) - \rho_{yx,measured}(0)\frac{\rho_{xx,measured}(B)}{\rho_{xx,measured}(0)}. \quad (1)$$

The effective medium model was fitted to the data with a MATLAB script that minimized the differences between the model values and the data values in both ρ_{xx} and ρ_{yx} and between their derivatives as a function of magnetic field strength. The matrix phase was modeled as a group of spherical crystallites. The impurity phase was modeled as a group of prolate spheroidal crystallites, with the ratio of the minor axis to the major axis set at 0.1. This number was determined from SEM micrographs (inset of Figure 1) showing the impurity phase. The effect of the 3% porosity on the transport measurements was estimated to be a 2% increase in ρ_{xx} and a 3% increase in ρ_{yx} using the effective medium model and treating the voids as spheres with zero conductivity. We therefore neglect the effect of the porosity on the transport measurements.

Stroud solved the electrostatic equations in a two-phase composite to derive the coherent potential approximation, which is given by[9]

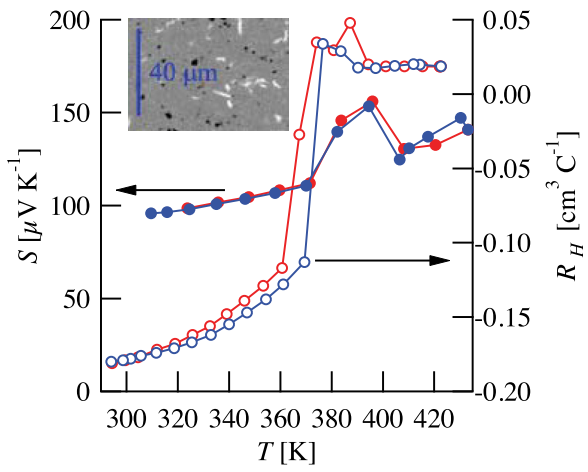

FIG. 1. Hall coefficient R_H (open symbols) and thermopower S (closed symbols) data below the phase transition in $Cu_{1.97}Ag_{0.03}Se$. The positive Seebeck coefficients indicate holes and the negative Hall coefficient indicates electrons as the majority carriers, showing the conflicting properties in this composite. Heating data are shown in red and cooling data in blue. The inset is an SEM micrograph of the material at room temperature.

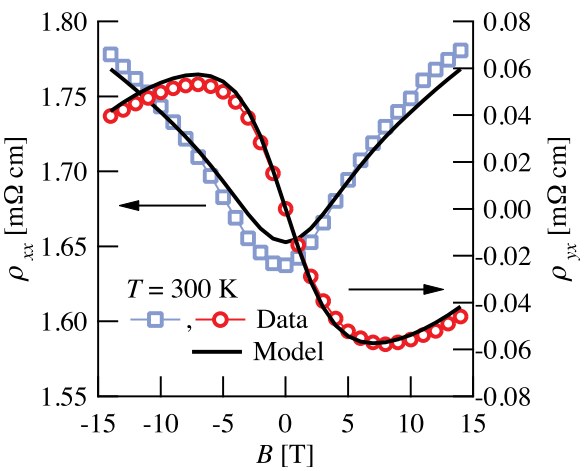

FIG. 2. Resistivity measurements as a function of magnetic field B at 300 K. A composite of two phases guarantees non-linear behavior in the magnetoresistance ρ_{xx} (open symbols) and the Hall effect ρ_{yx} (open symbols) due to the differences in the weighting of each phase by its electron mobility.

$$\vec{\vec{0}} = \sum_{i=1}^{2} f_i(\vec{\vec{\sigma}}_i - \vec{\vec{\sigma}}_e)(\vec{\vec{I}} - (\vec{\vec{\sigma}}_i - \vec{\vec{\sigma}}_e)\vec{\vec{\Gamma}}_i)^{-1}. \quad (2)$$

f_i is the volume fraction of phase i, $\vec{\vec{I}}$ is the identity matrix, and $\vec{\vec{\Gamma}}_i$ is the depolarization tensor of phase i, given by Eq. (S6).[9] $\vec{\vec{\Gamma}}_i$ relates the electric field inside a crystallite to that outside it and therefore depends on the shape of the crystallite and on the anisotropy of the effective conductivity tensor. $\vec{\vec{\sigma}}_e$ is the effective conductivity tensor, given by Eq. (S5). $\vec{\vec{\sigma}}_i$ is the conductivity tensor of phase i, given by[21]

$$\vec{\vec{\sigma}}_i = \sigma_{0,i}\begin{bmatrix} \frac{1}{1+(\mu_i B)^2} & \frac{\mu_i B}{1+(\mu_i B)^2} & 0 \\ \frac{-\mu_i B}{1+(\mu_i B)^2} & \frac{1}{1+(\mu_i B)^2} & 0 \\ 0 & 0 & 1 \end{bmatrix}. \quad (3)$$

$\sigma_{0,i}$ is the electrical conductivity at zero field, B is the magnetic field strength, and μ_i is the electron mobility. The magnetic field always points in the z-direction, and both phases are assumed to have zero longitudinal magnetoresistance, i.e., $\sigma_{i,zz}$ equals $\sigma_{0,i}$. $\vec{\vec{\sigma}}_i$ and $\vec{\vec{\sigma}}_e$, in general, are not isotropic, as evidenced by the different values of ρ_{xx} and ρ_{yx} in Figure 2 and in the supplementary material.[22] However, the behavior of $\vec{\vec{\sigma}}_i$ with B is completely specified by just two parameters, $\sigma_{0,i}$ and μ_i. Electronic bands in a phase are represented by tensors with the form of Eq. (3), and $\vec{\vec{\sigma}}_i$ for a multiband material is the sum of these tensors. Since Eq. (2) is a tensor equation, it contains two independent equations that can be numerically solved for $\sigma_{e,xx}$ and $\sigma_{e,xy}$, with $\sigma_{0,i}$ and μ_i as fitting parameters.

To first order, the volume-fraction weighted Hall conductivity of a single phase $\sigma_{i,xy}$ is $f_i\sigma_{0,i}\mu_i$, where f_i is the volume fraction of phase i. If the fractional contribution of the matrix phase to the Hall conductivity $|f_1\sigma_{0,1}\mu_1|/\Sigma|f_i\sigma_{0,i}\mu_i|$ is less than unity, and at least one of the phases has a magnetoresistance contribution $\mu_i B$ of order one, the impurity phase will make a measurable contribution to both the in-line and Hall resistivity, and both quantities will be nonlinear as a function of magnetic field, providing data from which the individual conductivity and mobility values can be extracted.

A representative measurement of the in-line resistivity ρ_{xx} and the Hall resistivity ρ_{yx} at 300 K, including the transport model, is shown in Figure 2. Data at higher temperatures can be found in the supplementary material.[22]

The in-line resistivity ρ_{xx} rises with positive and negative magnetic field, but its rate of change with B decreases with increasing B. This is referred to as saturating behavior. This is because each phase's contribution to ρ_{xx} is weighted by $1/(1+(\mu_i B)^2)$, meaning that as B increases, the contribution of the high mobility phase decreases, causing the rate of change of ρ_{xx} with B to decrease. The Hall resistivity ρ_{yx} exhibits linear behavior from 0 T to about +/−4 T. Again, this is because of the way ρ_{yx} is weighted with B. Each phase's contribution is weighted by $\mu_i B/(1+(\mu_i B)^2)$. At low values of B, the Hall resistivity will be dominated by the high mobility phase. As B increases, the high mobility phase will continue to dominate, but its contribution will decrease as the denominator $(1+(\mu_i B)^2)$ increases, leading to decreasing values of ρ_{yx} with B. Note, however, that if the Hall resistivity ρ_{yx} is converted to a Hall coefficient R_H according to $R_H = \rho_{yx}/B$, R_H stays negative across the entire range of B values, meaning that the n-type impurity phase is the majority contributor to the Hall effect in this material.

Each electronic band in each phase is characterized by a zero-field conductivity $\sigma_{0,i}$ and an electron mobility μ_i. We modeled the matrix phase as a single-band material and the impurity phase as a two-band material, for a total of six free parameters.

The estimates for $\sigma_{0,i}$ are shown in Table I. Ishiwata *et al.* used two conduction bands to model the resistivity tensor components of CuAgSe,[23] a strategy suggested by the nonlinear behavior of ρ_{xx} and ρ_{yx} with magnetic field observed in that work. For this reason, we have adopted the same strategy. The total conductivity of the impurity phase differs by up to 20% of that of CuAgSe. This suggests that while the impurity phase has the crystal structure of CuAgSe,[13] the impurity phase has a slightly different composition.

The estimates for the carrier mobility of each phase are shown in Table II. The units of 10^{-4} T^{-1} are numerically equal to the units of cm^2 V^{-1} s^{-1}, but it is more instructive to use inverse units of magnetic field strength to illustrate that the carrier mobility is a weighting factor for the electrical conductivity of each phase and each band.

The $\mu_i B/(1+(\mu_i B)^2)$ term reaches a maximum when $\mu_i B$ equals one, which for the high mobility band of the impurity phase is when $|B|$ is between 6 and 9 T, depending on temperature. At this value of $|B|$, ρ_{yx} reaches an extremum, and ρ_{xx} reaches an inflection point as the influence of the second phase declines due to saturation (see Figure 2).

Looking at Tables I and II reveals the cause of the nonlinear Hall effect in this material. At all temperatures studied, the material contains at least one band with a great enough mobility such that $\mu_i B$ is of order one; the contribution of the matrix phase to the Hall effect $|f_1\sigma_{0,1}\mu_1|/\Sigma|f_i\sigma_{0,i}\mu_i|$ is at most 85% and is as low as 50%. These two facts guarantee that the impurity phase will have an enormous influence on the Hall effect in the material, despite its making up less than 3% of the sample volume.

The electron mobility of the high-mobility band in the impurity phase is less than that reported for pure CuAgSe (Table II). This is because the impurity phase has a greater electron concentration that does pure CuAgSe (Figure 3), which leads to a lower electron mobility when electron scattering is dominated by acoustic phonons.[24]

Looking at the fit parameters together and as functions of temperature indicates that metal atoms move between the matrix and impurity phases. Computing the Hall carrier

TABLE I. Zero-field conductivity as a function of temperature.

$\sigma_{0,i}$ (S cm^{-1})	300 K	333 K	350 K	366 K	380 K
Impurity phase, band 1	1169	1101	1006	985	846
Impurity phase, band 2	147	120	148	83	34
Impurity phase, total	1316	1221	1154	1067	880
CuAgSe[23]	1305	1332	1208	1132	1052
Matrix	547	517	492	458	309
Cu_2Se[12]	853	768	731	650	497

TABLE II. Single band mobility as a function of temperature.

μ_i (10^{-4} T^{-1})	300 K	333 K	350 K	366 K	380 K
Impurity phase, band 1	−164	−167	−149	−138	−50
Impurity phase, band 2	−1458	−1504	−1090	−1235	−1178
CuAgSe[23]	−2191	…	…	…	…
Matrix	24	22	24	25	50
Cu_2Se[12]	13	12	11	11	10

concentration of the matrix with the relation $n_H = \sigma/e\mu$, where e is the elementary charge, and for the impurity phase with Eq. (4) (adapted from the equation for R_H[25] in by the relation $R_H = 1/n_H e$), we see that the carrier concentration of the matrix is reduced compared to that of Cu_2Se, and that of the impurity phase is increased relative to CuAgSe (Figure 3)

$$n_H = \frac{(\sigma_1 + \sigma_2)^2}{e(\sigma_1\mu_1 + \sigma_2\mu_2)}. \quad (4)$$

In the matrix, this must be due to Ag dissolving in the lattice. This is supported by X-ray diffraction by Brown *et al.*[12] in which the reflections of $Cu_{1.97}Ag_{0.03}Se$ are shifted to smaller values of 2Θ, indicating a larger lattice, which is consistent with the larger Ag cations located on vacant Cu sites.[26] Ordinarily these vacant sites create holes in Cu_2Se; an Ag atom on such a site donates an electron and reduces the number of positive charge carriers. Ag has been shown to reduce the carrier concentration in Cu_2Se,[13] further supporting the idea that the matrix is Ag-doped Cu_2Se. In general, because the impurity phase dissolves into the matrix at higher temperatures, slightly different compositions of the cation ratios are not surprising.

The matrix phase and Cu_2Se both show a gradual decline of carrier concentration with temperature, but between 366 K and 380 K the carrier concentration of the matrix drops more sharply than does the carrier concentration of Cu_2Se. In this temperature range, Ag becomes more soluble in the matrix. The introduction of more Ag into the matrix fills more holes in the valence band of the matrix, reducing the carrier concentration. This is consistent with the jump in the matrix phase mobility, as the mobility tends to increase as the carrier concentration decreases.

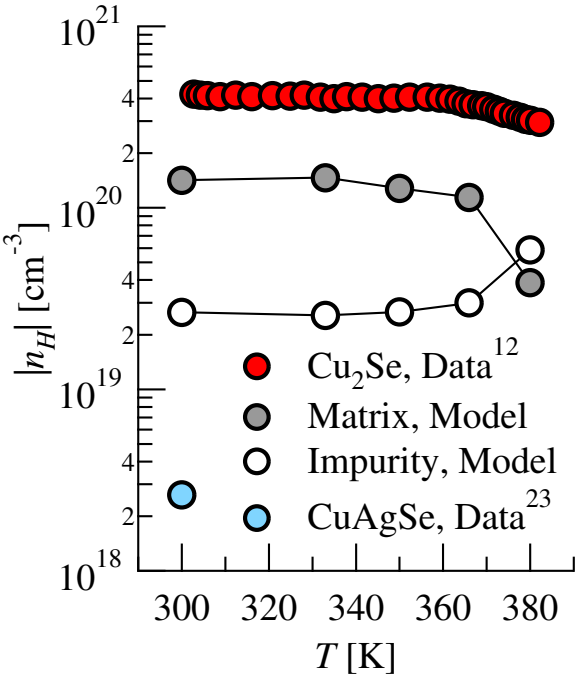

FIG. 3. Hall carrier concentrations measured on pure Cu_2Se and CuAgSe and extracted from the model for the matrix and impurity phases.

The increase in the Hall carrier concentration of the impurity phase relative to CuAgSe could be due to an elevated cation to anion ratio. The dependence of the Hall carrier concentration of the impurity phase on temperature is more complicated because of the mobility-dependent contribution of each band. It is difficult to distinguish from the model parameters in Tables I and II the effects of temperature, the mass exchange between the phases, and the changing energy difference between the two bands. However, Figure 3 shows that the Hall carrier concentration of the impurity phase gradually rises and then jumps between 366 K and 380 K. Between these two temperatures, the conductivity of band 1 drops much less than does the conductivity of band 2 (Table II). This means that the carrier concentration will be more influenced by band 1, the band containing more carriers, and that the overall Hall carrier concentration will increase.

The classical influence of an impurity phase on the resistivity tensor of $Cu_{1.97}Ag_{0.03}Se$ and the interest in using impurity phases to create beneficial quantum effects in thermoelectrics drove us to introduce effective medium theory as a tool for optimizing phase-segregated thermoelectrics. We have shown that useful information on each band in each phase can be gathered by measuring the independent components of the resistivity tensor at high magnetic fields. In combination with X-ray diffraction and classic thermoelectric characterization techniques, we present a powerful tool to model and understand multiphase behavior in semiconductors, in order to optimize materials compositions for high figure of merit thermoelectrics, such as composites of Sb_2Te_3 and PbTe,[27] Ag_2Te and PbTe,[4] In_2Te_3 and Bi_2Te_3,[28] or $AgSbTe_2$ with nanodot inclusions,[6] as well as to quantify the negative effects of impurities.

T.W.D., D.R.B., and G.J.S. are grateful for the support of the AFOSR MURI program under FA9550-12-1-0002. D.R.B. acknowledges the support of the Resnick Institute. B.C.M. gratefully acknowledges financial support through start-up funding provided by the Dana and David Dornsife College of Letters and Sciences at the University of Southern California. W.G.Z. also acknowledges the support of a fellowship within the Postdoc-Program of the German Academic Exchange Service (DAAD).

[1]N. A. Heinz, T. Ikeda, Y. Pei, and G. J. Snyder, Adv. Funct. Mater. **24**(15), 2135 (2014).
[2]M. Schwall, L. M. Schoop, S. Ouardi, B. Balke, C. Felser, P. Klaer, and H. J. Elmers, Adv. Funct. Mater. **22**(9), 1822 (2012).
[3]M. Zebarjadi, G. Joshi, G. Zhu, B. Yu, A. Minnich, Y. Lan, X. Wang, M. Dresselhaus, Z. Ren, and G. Chen, Nano Lett. **11**(6), 2225 (2011).
[4]Y. Pei, N. A. Heinz, A. D. LaLonde, and G. J. Snyder, Energy Environ. Sci. **4**(9), 3640 (2011).
[5]J. P. Heremans, C. M. Thrush, and D. T. Morelli, Phys. Rev. B **70**(11), 115334 (2004).

[6]K. F. Hsu, S. Loo, F. Guo, W. Chen, J. S. Dyck, C. Uher, T. Hogan, E. K. Polychroniadis, and M. G. Kanatzidis, Science **303**, 818 (2004).
[7]D. J. Bergman and O. Levy, J. Appl. Phys. **70**(11), 6821 (1991).
[8]W. G. Zeier, A. LaLonde, Z. M. Gibbs, C. P. Heinrich, M. Panthöfer, G. J. Snyder, and W. Tremel, J. Am. Chem. Soc. **134**(16), 7147 (2012).
[9]D. Stroud, Phys. Rev. B **12**(8), 3368 (1975).
[10]A. Minnich and G. Chen, Appl. Phys. Lett. **91**(7), 073105 (2007).
[11]C. W. Nan, R. Birringer, D. R. Clarke, and H. Gleiter, J. Appl. Phys. **81**(10), 6692 (1997).
[12]D. R. Brown, T. Day, K. A. Borup, S. Christensen, B. B. Iversen, and G. J. Snyder, APL Mater. **1**, 052107 (2013).
[13]T. W. Day, K. A. Borup, T. Zhang, F. Drymiotis, D. R. Brown, X. Shi, L. Chen, B. B. Iversen, and G. J. Snyder, Mater. Renewable Sustainable Energy **3**, 26 (2014).
[14]B. Xu and M. J. Verstraete, Phys. Rev. Lett. **112**, 196603 (2014).
[15]C. M. Jaworski, M. D. Nielsen, H. Wang, S. N. Girard, W. Cai, W. D. Porter, M. G. Kanatzidis, and J. P. Heremans, Phys. Rev. B **87**(4), 045203 (2013).
[16]V. Jovovic and J. P. Heremans, Phys. Rev. B **77**(24), 245204 (2008).
[17]S. Ballikaya, H. Chi, J. R. Salvador, and C. Uher, J. Mater. Chem. A **1**, 12478–12484 (2013).
[18]K. Kashida and J. Akai, J. Phys. C: Solid State Phys. **21**(31), 5329 (1988).
[19]K. A. Borup, E. S. Toberer, L. D. Zoltan, G. Nakatsukasa, M. Errico, J. P. Fleurial, B. B. Iversen, and G. J. Snyder, Rev. Sci. Instrum. **83**(12), 123902 (2012).
[20]M. Levy and M. P. Sarachik, Rev. Sci. Instrum. **60**(7), 1342 (1989).
[21]V. Guttal and D. Stroud, Phys. Rev. B **73**(8), 085202 (2006).
[22]See supplementary material at http://dx.doi.org/10.1063/1.4897435 for a more complete derivation of the effective medium model, a sensitivity analysis of the model, and fits of the model to the data at other temperatures.
[23]S. Ishiwata, Y. Shiomi, J. S. Lee, M. S. Bahramy, T. Suzuki, M. Uchida, R. Arita, Y. Taguchi, and Y. Tokura, Nat. Mater. **12**(6), 512 (2013).
[24]A. H. Wilson, *The Theory of Metals* (The Syndics of the Cambridge University Press, 1958).
[25]A. F. May and G. J. Snyder, in *Thermoelectrics and its Energy Harvesting*, edited by D. M. Rowe (CRC Press, 2012).
[26]M. K. Balapanov, R. K. Ishembetov, Y. K. Yulaeva, and R. A. Yakshibaev, Russ. J. Electrochem. **47**(12), 1337 (2011).
[27]T. Ikeda, N. J. Marolf, K. Bergum, M. B. Toussaint, N. A. Heinz, V. A. Ravi, and G. J. Snyder, Acta Mater. **59**(7), 2679–2692 (2011).
[28]N. A. Heinz, T. Ikeda, and G. J. Snyder, Acta Mater. **60**(11), 4461 (2012).